Available online at www.sciencedirect.com
SCIENCE DIRECT
ELSEVIER
Journal of Physics and Chemistry of Solids 67 (2006) 745–750
JOURNAL OF PHYSICS AND CHEMISTRY OF SOLIDS
www.elsevier.com/locate/jpcs

EPR study of Cu(II) dopant ions in single crystals of bis(L-asparaginato)Zn(II)

R.C. Santana [a,*], M.G. Santos [a], R.O. Cunha [a], K.D. Ferreira [a], J.F. Carvalho [a], R. Calvo [b]

[a] *Instituto de Física, Universidade Federal de Goiás, Campus Samambaia, CP 131, 74001-970 Goiânia (GO), Goias, Brazil*
[b] *Departamento de Física, Facultad de Bioquímica y Ciencias Biológicas, Universidad Nacional del Litoral, INTEC (CONICET-UNL), Güemes 3450, 3000 Santa Fe, Argentina*

Received 16 August 2005; received in revised form 22 November 2005; accepted 25 November 2005

Abstract

We report an electron paramagnetic resonance (EPR) study at 33.9 GHz and room temperature of oriented single crystal samples of bis(L-asparaginato)Zn(II) doped with Cu(II). The variation of the spectra with magnetic field orientation was measured in three crystal planes (a^*b, bc and a^*c, with $\boldsymbol{a}^* = \boldsymbol{b} \times \boldsymbol{c}$). These spectra display two groups of four peaks arising from the hyperfine interaction with the $I_{Cu} = 3/2$ nuclear spins of copper. They were assigned to Cu(II) ions in two lattice sites related by a 180° rotation around the $\boldsymbol{b}$-crystal axis. The $\boldsymbol{g}$ and hyperfine coupling ($\boldsymbol{A}$) tensors of the Cu(II) ions were evaluated from the single crystal data. Some indeterminacy in the assignment of the signals was avoided measuring the EPR spectrum of a powder sample. Their principal values are $g_1 = 2.060(1)$, $g_2 = 2.068(2)$, $g_3 = 2.283(2)$, and $A_1 \approx 0.1 \times 10^{-4}$, $A_2 = 13 \times 10^{-4}$ and $A_3 = 165 \times 10^{-4}$ cm^{-1}. The eigenvectors corresponding to g_3 and A_3 are coincident within the experimental error; the other eigenvectors are rotated 5.6° in the perpendicular plane. Considering the crystal structure of bis(L-asparaginato)Zn(II), our EPR results indicate that the Cu(II) impurities replace Zn(II) ions in the host crystal. We propose a molecular model based on the EPR data and the structural information, and analyse the results comparing the measured values with those obtained in similar systems.

Keywords: D. Electron paramagnetic resonance (EPR)

1. Introduction

Electron paramagnetic resonance (EPR) is a powerful technique to study the electronic structure of transition ions. It has been applied to study paramagnetic impurities introduced in diamagnetic metal compounds, when the spectra have narrow lines and often show hyperfine structure with the nuclear spins of the paramagnetic metal ion and the ligands. In these investigations, the data provide information about the electronic structure of the impurity ions, their interactions with the diamagnetic environment and in some cases also about vibronic couplings and dynamical Jahn–Teller effects [1,2].

Metal compounds of amino acids and peptides are appropriate model systems for metal ions in proteins. In pure paramagnetic compounds the exchange interactions between the metal ions average out most of the structure of the EPR spectra. Information about the electronic structure and about the interactions involving a single metal ion has been obtained with the paramagnetic ions introduced as impurities in isostructural diamagnetic metal–amino acid compounds, generally the corresponding Zn compounds. As a consequence of its higher experimental and theoretical simplicity, copper(II) is the best understood transition metal ion. Detailed single crystal EPR studies of copper introduced as dopant ions in the diamagnetic Zn compounds of the amino acids L-leucine [3], L-glutamic acid [4], L-alanine [5], L-aspartic acid [6,7] and D,L-histidine [8] have been reported. The results for diaqua (L-aspartate)Zn(II) hydrate:Cu(II) [6,7] and for bis(D,L-histidine)Zn(II) pentahydrate:Cu(II) [8] display important contributions arising from vibronic couplings and Jahn–Teller effects. They produce large temperature variations of the EPR spectral parameters, and displacements of the g-factors and hyperfine parameters from those expected for copper in square planar or distorted octahedral coordination. Meanwhile, the EPR spectra of Cu ions in other Zn–amino acid hosts [3–5] display negligible changes with temperature of the EPR spectra. Also, their g-factors and hyperfine coupling parameters have approximate axial symmetry.

* Corresponding author. Tel./fax: +55 62 3521 1029.
E-mail address: santana@if.ufg.br (R.C. Santana).

0022-3697/$ - see front matter © 2005 Elsevier Ltd. All rights reserved.
doi:10.1016/j.jpcs.2005.11.006

No data seem to exist for copper ions introduced in diamagnetic metal–asparagine compounds (asparagine is the beta-amido derivative of aspartic acid) and in this work we report an EPR study of copper dopant ions in powder and single crystals of bis(L-asparaginato)Zn(II) $Zn(COONH_2\text{-}CHCH_2CONH_2)_2$, to be called Zn(L-asn)$_2$ whose crystal structure was reported by Stephens et al. [9]. Zn(L-asn)$_2$ is monoclinic, space group $P2_1$, with unit-cell dimensions $a=12.323(1)$, $b=5.027(2)$, $c=9.702(2)$ Å, and $\beta=99.12(4)^\circ$, and two formula units per unit cell ($Z=2$). As shown in Fig. 1, where the labelling of the atoms was taken from the Cambridge Structural Database [10] and the hydrogen atoms are omitted for clarity, the Zn ion is in a distorted octahedral site coordinated to the carboxylic O atoms and to the α-amino N atoms of two L-asparagine molecules in a *trans* square planar configuration (distances Zn–O 2.086 and 2.102 Å, Zn–N 2.071 and 2.092 Å). In the axial direction, there are two carbonyl O atoms from neighbouring molecules at 2.28 and 2.48 Å, completing a square bipyramid. In comparison, the equatorial coordination of the Cu(II) ion in the pure complex bis(L-asparaginato)Cu(II) [11,12] is similar to that in the Zn compound; the copper ion is also bonded to two molecules of the amino acid which enter as bidentate ligands through the amino nitrogen and the carboxylate oxygen. However, in the copper compound the apical ligands of the distorted square pyramidal coordination are amido O atoms from neighbour amino acid molecules at 2.229 and 2.885 Å.

In this work, we report an EPR study of Cu(II) introduced as dopant ions in Zn(L-asn)$_2$ crystals. Single crystal EPR measurements allow obtaining the Zeeman and anisotropic hyperfine interactions. The results are discussed in terms of the electronic structure of the copper ions in Zn(L-asn)$_2$ and compared with those obtained for copper in other amino acid compounds.

2. Experimental details

2.1. Sample preparation

The amino acid L-asparagine obtained from Ajinomoto Co. was used without further purification. The complex Zn(L-asn)$_2$ was crystallized before doping with copper. The crystals were obtained from aqueous solution of L-asparagine (37.0 mmol), zinc chloride ($ZnCl_2$, 18.5 mmol) and NaOH (37.0 mmol, to obtain solutions with neutral pH) in 100 ml of water. After few days of slow solvent evaporation small colourless thin single crystal plates showing *bc* faces elongated along the ***b***-axis precipitated. They were identified using X-ray diffraction as the complex Zn(L-asn)$_2$ reported by Stephens et al. [9]. Copper-doped bis(L-asparaginato)zinc crystals (Zn(L-asn)$_2$:Cu(II)) were grown by solvent evaporation of an aqueous solution of Zn(L-asn)$_2$ with 0.5 wt% of $CuSO_4\cdot 5H_2O$. Small plate-shaped crystals of Zn(L-asn)$_2$:Cu(II) with the same habit as the pure crystals and showing a slight bluish coloration were obtained. According to X-ray diffraction measurements the doped crystals have the same lattice parameters as the pure crystals, as expected from the low impurity concentration.

2.2. EPR measurements

We used a Bruker ESP-300 spectrometer operating at 33.9 GHz, a cylindrical microwave cavity with 100 kHz field

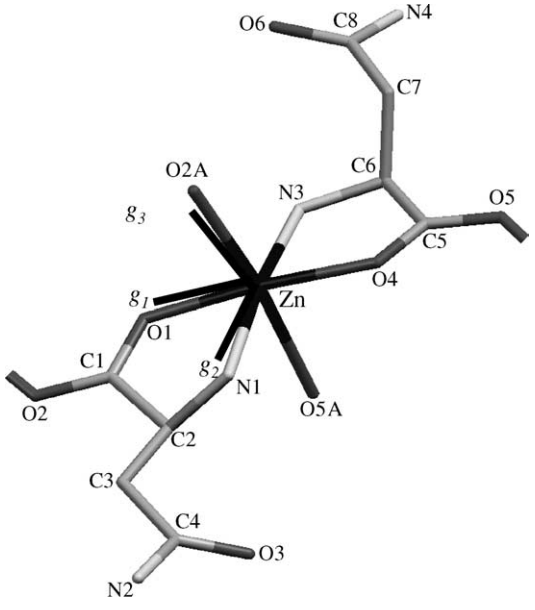

Fig. 1. Molecular structure of Zn(L-asn)$_2$ as obtained from the crystallographic data of Ref. [9], including the principal directions of the ***g*** tensor of the copper ions. The proximity of these directions to the molecular axes supports that Cu(II) impurities replace the Zn(II) ions in the structure of Zn(L-asn)$_2$.

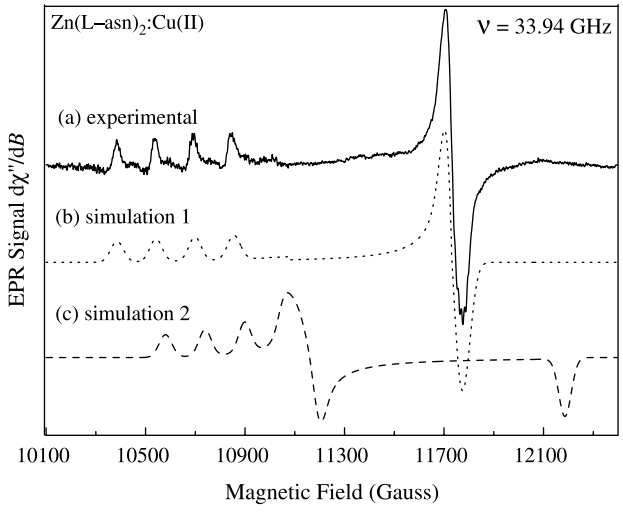

Fig. 2. (a) EPR spectra at 300 K observed for a powdered sample of copper doped Zn(L-asn)$_2$. Very small changes of the EPR spectrum with temperature are observed between 77 and 300 K. (b) Simulated spectrum obtained with the values of the parameters given in Table 1, representing the correct solution of the spin Hamiltonian of Cu:Zn(L-asn)$_2$. (c) Spectrum simulated with the *g*-values: $g_1=1.9909$; $g_2=2.1787$ and $g_3=2.2416$, and corresponding values for the components of the ***A*** tensor, a solution which satisfies the single crystal data, but does not show the expected axial symmetry of the ***g***-tensor.

modulation, and a rotating magnet. The magnetic field was calibrated using diphenylpicrylhydrazyl (DPPH, $g=2.0036$) as a field marker positioned close to the sample. The measurements were made at room temperature in powdered samples (see Fig. 2a), and in oriented single crystals of Cu doped Zn(L-asn)$_2$, at 33.9 GHz. The powdered sample was obtained by crushing crystals of quality similar to those used in the single crystal EPR measurements. The microwave power and modulation amplitude were 12.6 mW and 2.8 G, respectively. For the powdered sample, EPR spectra observed at temperatures between 77 and 300 K show little positional changes from that observed at room temperature.

The orientation of the crystals was attained by gluing a *bc* plane of the plates to a face of a cleaved KBr cubic single crystal holder (Fig. 3a) defining a set of orthogonal ***x***,***y***,***z***-axes, with the $\boldsymbol{a}^*=\boldsymbol{b}\times\boldsymbol{c}$, ***b*** and ***c*** crystal directions of the sample along the ***x***, ***y*** and ***z*** directions of the holder, respectively. This sample holder was mounted on the horizontal plane at the top of a pedestal in the axis of the cavity. The EPR spectra were recorded with the magnetic field B at 5° intervals in a range of 180°, in three orthogonal planes a^*b, a^*c and bc. The positions of the crystal axes in the a^*b, and bc planes were determined within ~1° from the symmetry properties of the monoclinic ***b***-axis. In the *ac* plane, they were determined by a least squares procedure, considering the data in three orthogonal planes.

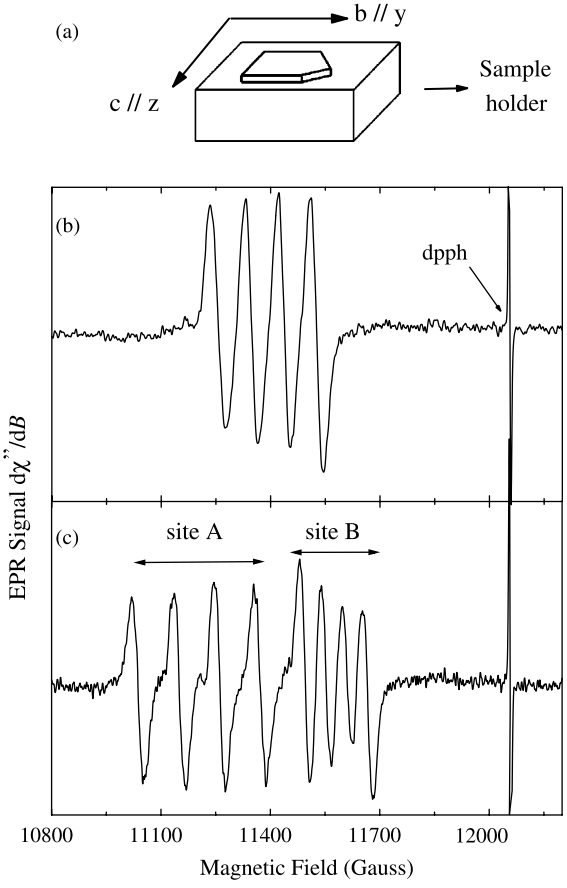

Fig. 3. (a) View of the sample holder and sample used in the single-crystal EPR experiments. The positions of the crystal axes ***b*** and ***c*** in the ***xyz***-axes of the holder are indicated. The $\boldsymbol{a}^*//\boldsymbol{z}$-axis is normal to the sample plane. (b) and (c) EPR spectra of a single-crystal sample of Zn(L-asn)$_2$:Cu observed at 33.9 GHz. (b) Four lines spectrum observed for $\boldsymbol{B}//\boldsymbol{b}$. (c) Eight lines spectrum observed for ***B*** at 20° from the ***b***-axis in the *bc*-plane.

2.3. Spectral simulations

EPR spectra of powder samples were simulated using EasySpin [13,14]. The simulations consider the presence of the two natural copper isotopes ($I=3/2$) with their natural abundances. Isotropic Gaussian derivative line shape was proposed in all cases.

3. Analysis of the EPR results

The observed EPR spectrum of powdered Zn(L-asn)$_2$:Cu shown in Fig. 2a displays in the low field region resolved hyperfine structure with the copper nucleus, as expected in samples doped with small concentrations of copper in tetragonal symmetry [15].

Fig. 3b and c displays EPR spectra of a single crystal sample of Cu:Zn(L-asn)$_2$ with the magnetic field applied along the ***b***-axis, and at 20° from the ***b***-axis in the *bc* plane, respectively. Gaussian derivative line shapes are observed. With the magnetic field along the ***b***-axis or in the a^*c plane, one observes one four-line resonance set (Fig. 3b), corresponding to the hyperfine structure of the $S=1/2$ Cu(II) ions interacting with the $I_{Cu}=3/2$ nuclear spins of two copper isotopes, having similar magnetic moments. Two four-line sets are observed for other orientations of the magnetic field (Fig. 3c). This result is expected from the crystal structure of Zn(L-asn)$_2$ if copper ions occupy the Zn sites of the unit cell. The magnetic field positions of the lines were calculated with a least-squares fit of the field derivative of four or eight Gaussian line shapes to the observed signal. No resolved ligand superhyperfine interactions are observed for any orientation $\boldsymbol{h}=\boldsymbol{B}/|\boldsymbol{B}|$ of the magnetic field.

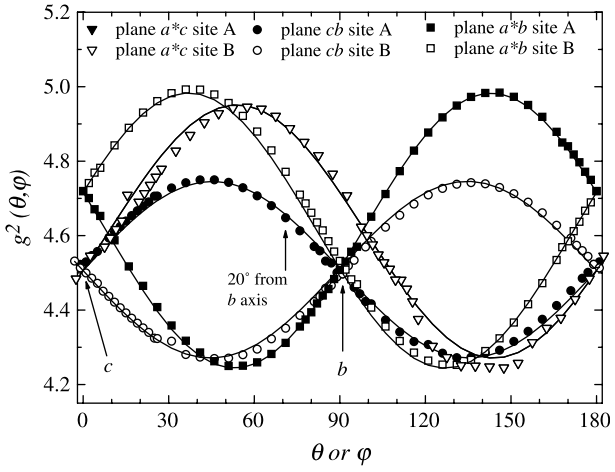

Fig. 4. Angular variation of $g^2(\theta,\phi)$ in the planes a^*b, a^*c, bc. The symbols represent the values obtained from the data. The solid lines were obtained with the components of the $\boldsymbol{g}\cdot\boldsymbol{g}$ tensor given in Table 1. The arrows indicate the orientations where the spectra shown in Fig. 3b and c were obtained.

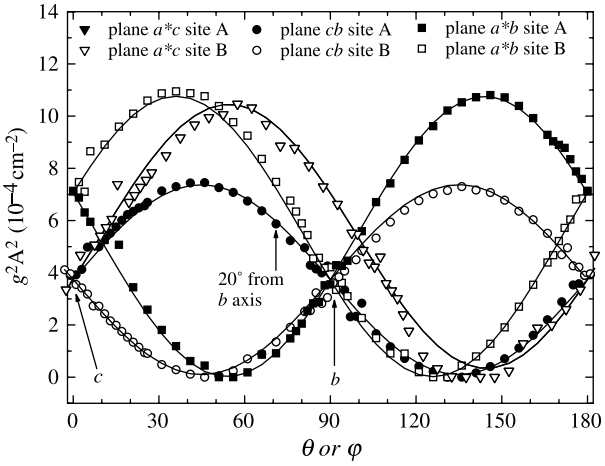

Fig. 5. Angular variation of $g^2A^2(\theta,\phi)$ in three crystallographic planes. The solid lines were obtained with the components of the $\boldsymbol{g}$ and $\boldsymbol{A}$ tensors given in Table 1.

The spin Hamiltonian describing the spectra of a Cu(II) spin and the hyperfine interaction with the copper nucleus in a site α of the Zn(L-asn)$_2$ lattice (α = A, B) is

$$\boldsymbol{H}_\alpha = \mu_B \boldsymbol{S}_\alpha \cdot \boldsymbol{g}_\alpha \cdot \boldsymbol{B} + \boldsymbol{S}_\alpha \cdot \boldsymbol{A}_\alpha \cdot \boldsymbol{I}_\alpha \quad (1)$$

where μ_B is the Bohr magneton and $\boldsymbol{B}$ is the applied magnetic field. $\boldsymbol{S}_\alpha$ ($S=1/2$), $\boldsymbol{I}_\alpha$ ($I=3/2$), $\boldsymbol{g}_\alpha$ and $\boldsymbol{A}_\alpha$ are, respectively, the electronic spin of the copper ions, the nuclear spin of the copper nuclei, the $\boldsymbol{g}$-tensor and the copper hyperfine tensor for a copper ion in the α site. The angular dependence of $g^2(\theta,\phi) = \boldsymbol{h}\cdot\boldsymbol{g}\cdot\boldsymbol{g}\cdot\boldsymbol{h}$ and $g^2A^2(\theta,\phi) = \boldsymbol{h}\cdot\boldsymbol{g}\cdot\boldsymbol{A}\cdot\boldsymbol{A}\cdot\boldsymbol{g}\cdot\boldsymbol{h}$, calculated from the data with the magnetic field in the planes a^*b, a^*c and bc are shown in Figs. 4 and 5. These results demonstrate that the copper ions are in two symmetry related sites in the structure of Zn(L-asn)$_2$, chemically equal but magnetically non-equivalent, related by 180° rotation around the $\boldsymbol{b}$-axis. The components of the $\boldsymbol{g}$ and $\boldsymbol{A}$ tensors were obtained with an iterative method reported previously [16] that uses a perturbative expansion of the spin Hamiltonian up to second order reported by Weil [17]. In this method, the positions $B(m_{Cu})$ of the EPR transitions with $I_z = m_{Cu}$ ($m_{Cu} = \pm 1/2,\ \pm 3/2$) and $S = \pm 1/2$ for the magnetic field along $\boldsymbol{h}$ are calculated for each α site using:

$$\begin{aligned} B(m_{Cu}) = &\{h\nu_0/g\mu_B - K_{Cu}m_{Cu}/g\mu_B - [(\mathrm{Tr}(A_{Cu}^2) - k_{Cu}^2) \\ &I_{Cu}(I_{Cu}+1)]/(4g_\alpha^2\mu_B^2 B)\} + \sum (m_{Cu}^2/2g^2\mu_B^2 B) \\ &\times \{1/2\mathrm{Tr}(A_{Cu}^2) + K_{Cu}^2 - 3/2k_{Cu}^2\} \end{aligned} \quad (2)$$

The first two terms on the right side of Eq. (2) correspond to the solution in first order approximation, and the other ones to those in second order approximation, ν_0 is the microwave frequency, h is the Planck constant, and $g = (\boldsymbol{h}\cdot\boldsymbol{g}\cdot\boldsymbol{g}\cdot\boldsymbol{h})^{1/2}$, $gK_{Cu} = (\boldsymbol{h}\cdot\boldsymbol{g}\cdot\boldsymbol{A}_{Cu}\cdot\boldsymbol{A}_{Cu}\cdot\boldsymbol{g}\cdot\boldsymbol{h})^{1/2}$ and $gK_{Cu}k_{Cu} = (\boldsymbol{h}\cdot\boldsymbol{g}\cdot\boldsymbol{A}_{Cu}\cdot\boldsymbol{A}_{Cu}\cdot\boldsymbol{A}_{Cu}\cdot\boldsymbol{A}_{Cu}\cdot\boldsymbol{g}\cdot\boldsymbol{h})^{1/2}$, are the projections of the tensors $\boldsymbol{g}$, $\boldsymbol{gA}_{Cu}$, and $\boldsymbol{gA}_{Cu}\boldsymbol{A}_{Cu}$ along the direction $\boldsymbol{h}$ of the applied field, and Tr denote the trace of the tensor. There are four different possibilities to assign the two groups of resonances observed in the three studied planes, giving two pairs of sets of values for the spin Hamiltonian parameters. Each pair gives the same eigenvalues for the $\boldsymbol{g}$ and $\boldsymbol{A}$ tensors, and eigenvectors related by a C_2 rotation around the $\boldsymbol{b}$-axis. Simulations of the powder EPR spectrum using EasySpin [13,14] were performed for each pair of sets (Fig. 2b and c). One pair, displaying axial symmetry for the $\boldsymbol{g}$-tensor, reproduces the observed powder EPR spectrum at 300 K (see Fig. 2b). It was considered the correct solution for the A and B lattice sites for the copper impurities (see discussion of a similar situation in [6]). The other pair do not have a $\boldsymbol{g}$-tensor with axial symmetry and do not reproduce the observed powder spectrum (see Fig. 2c) and thus it is not a feasible choice. Table 1 contains the values of the components of the $\boldsymbol{g}$- and hyperfine tensors calculated from the single crystal data that reproduce the powder spectrum. It includes their eigenvalues and eigenvectors referred to the orthogonal set of laboratory

Table 1
Components of the $\boldsymbol{g}^2(a)$ and $\boldsymbol{g}^2\boldsymbol{A}^2$ tensors (b) calculated from a least squares analysis of the single crystal EPR spectra of Cu(II) impurities in Zn(L-asn)$_2$ (values in Figs. 2 and 3), (c) and (d) Eigenvalues and eigenvectors of the tensors $\boldsymbol{g}$ and $\boldsymbol{A}$.

(a) $\boldsymbol{g}^2$ tensor	
$(\boldsymbol{g}^2)_{xx} = 4.716(7)$	$(\boldsymbol{g}^2)_{xy} = \pm 0.355(5)$
$(\boldsymbol{g}^2)_{yy} = 4.511(9)$	$(\boldsymbol{g}^2)_{xz} = 0.323(1)$
$(\boldsymbol{g}^2)_{zz} = 4.506(3)$	$(\boldsymbol{g}^2)_{yz} = \pm 0.237(5)$
(b) $\boldsymbol{g}^2\boldsymbol{A}^2$ tensor ($\times 10^{-4}$ cm^{-2})	
$(\boldsymbol{g}^2\boldsymbol{A}^2)_{xx} = 6.79(9)$	$(\boldsymbol{g}^2\boldsymbol{A}^2)_{xy} = \pm 5.03(8)$
$(\boldsymbol{g}^2\boldsymbol{A}^2)_{yy} = 3.42(9)$	$(\boldsymbol{g}^2\boldsymbol{A}^2)_{xz} = 4.71(8)$
$(\boldsymbol{g}^2\boldsymbol{A}^2)_{zz} = 4.13(9)$	$(\boldsymbol{g}^2\boldsymbol{A}^2)_{yz} = \pm 3.34(8)$
(c) Eigenvalues $\boldsymbol{g}$-tensor	*Eigenvectors $\boldsymbol{g}$-tensor*
$g_1 = 2.060(1)$	$(0.642(1), \mp\mu 0.760(3), -0.104(3))$
$g_2 = 2.068(2)$	$(\pm 0.322(5), 0.389(2), \mp\mu 0.863(6))$
$g_3 = 2.283(2)$	$(0.696(1), \pm 0.520(6), 0.494(6))$
(d) Eigenvalues $\boldsymbol{A}$-tensor ($\times 10^{-4}$ cm^{-1})	*Eigenvectors $\boldsymbol{A}$-tensor*
$A_1 \approx 0.1(2)$	$(0.592(1), \mp 0.801(3), -0.034(3))$
$A_2 = 13(2)$	$(\pm 0.394(2), 0.330(5), \mp\mu 0.858(1))$
$A_3 = 165(2)$	$(0.699(3), \pm 0.499(5), 0.513(1))$

The double signs correspond to sites α = A and B. The eigenvectors are given in the $\boldsymbol{xyz} \equiv \boldsymbol{a^*bc}$.

Table 2
Spin Hamiltonian parameters measured at temperature T for Cu(II) in Zn(L-asn)$_2$ and in related Zn–amino acid compounds (A in units of 10^{-4} cm^{-1} and angle in degrees) in single crystal EPR experiments.

Sample	T (K)	g_1	g_2	g_3	A_1	A_2	A_3	Angle	Ref.
Zn(L-asn)$_2$	300	2.060	2.068	2.283	0.1	13	165	5	–[a]
Zn(L-leu)$_2$	300	2.055	2.066	2.273	0	11	167.3	10	[3]
Zn(L-glu)	300	2.053	2.089	2.345	39	1	131		[4]
Zn(L-ala)$_2$	300	2.053	2.074	2.265	0	15	169	7	[5]
Zn(L-asp)	77	2.028	2.144	2.351	58	3.6	114.5		[6]
Zn(L-asp)	300	2.0377	2.1701	2.3127	61.5	20.5	87.8		[6]
Zn(D,L-his)$_2$	80	2.057	2.081	2.269	0	37	167	8	[8]
Zn(D,L-his)$_2$	298	2.071	2.124	2.204	25	48	120	8	[8]

[a] This work.

axes $\boldsymbol{xyz} \equiv \boldsymbol{a^*bc}$, which provide the orientation of the $\boldsymbol{g}$ and $\boldsymbol{A}$ tensors in the system of crystal axes. The double signs in the eigenvectors indicate the symmetry related sites A and B, related by a C_2 rotation around $\boldsymbol{b}$. The solid lines in Figs. 4 and 5 were calculated with the values of these components.

4. Discussion and conclusions

The $3d^9$ electron configuration of the Cu(II) ion is treated as a $3d^1$ hole configuration with effective electron spin $S=1/2$, and nuclear spin $I_{Cu}=3/2$ for each natural isotope. Our EPR results in single crystals give information about the geometry and electronic properties of copper impurities in Zn(L-asn)$_2$, indicating that copper ions occupy the Zn sites in the structure. The powder spectrum was used to decide a proper assignment of the resonances observed in three perpendicular crystal planes. It is important to point out that no changes of the powder spectrum with temperature were observed between 77 and 300 K. This indicates absence of vibronic contributions, which usually changes the EPR spectra in this temperature range. This is similar to what was found for Cu impurities in Zn(L-leu)$_2$ [3], Zn(L-glu) [4] and Zn(L-ala)$_2$ [5] (see Table 2), cases where the environment of the replaced Zn ion in the Zn compound is similar to the environment of the Cu ion in the corresponding Cu compound. In the cases where this environment is different, as occurs for the Zn and Cu complexes of aspartic acid [6] and histidine [8], important vibronic effects were observed (see Table 2) indicating instabilities of the bonding of Cu impurities in a Zn amino acid compound appear when the natural environments of the two ions bonded to the amino acid are different. This information is valuable, but still needs more experimental confirmations.

Eigenvalues and eigenvectors of the tensors $\boldsymbol{g}$ and $\boldsymbol{A}$, listed in Table 1 for Zn(L-asn)$_2$:Cu(II), reflect the approximate axial symmetry characteristic of copper ions sites having an approximately square planar *trans* array of O and N ligands [15]. The principal values g_3 and A_3 have nearly parallel eigenvectors (1.6°), indicating a $d(x^2-y^2)$ ground orbital state for the unpaired electron, this orbital is associated to the Cu(II) ion in a elongated octahedral configuration of negatively charged ligands [15], as for the structure of Zn(L-asn)$_2$. The Zn(L-asn)$_2$ molecule [9] displayed in Fig. 1 includes the principal directions of the $\boldsymbol{g}$ tensor of the copper impurities obtained from the single crystal EPR data. The angle between the eigenvector corresponding to g_3 and the normal to the copper (zinc) equatorial plane defined by the O4, O1, N1 and N3 nearest ligands calculated from the structural information [9] is $(5\pm1)°$. This small angle indicates that the Cu dopant ions occupy the Zn positions in Zn(L-asn)$_2$ and that the local distortion of the Zn site upon Cu substitution is small. Probably, the apical ligands to Cu(II) ions in Zn(L-asn)$_2$ are the carbonyl oxygen atoms (as for Zn(II) ions [9]), and not the amido oxygens, as observed in Cu(L-asn)$_2$ [11,12]. The absence of resolved superhyperfine interactions in Zn(L-asn)$_2$:Cu may be attributed to longer distances between the metallic centre (Zn/Cu) and ligands N for Zn(L-asn)$_2$ than for the others compounds.

Acknowledgements

The authors acknowledge financial support from Conselho Nacional de Desenvolvimento Científico e Tecnológico (CNPq) and Fundação de Apoio à Pesquisa da Universidade Federal de Goiás (FUNAPE) in Brazil, and CAI+D from Universidad Nacional del Litoral, AMPCyT (PICT 06-13872) and CONICET (PIP 5274), in Argentina. We thank to the Spanish Research Council (CSIC) for providing us with free-of-charge licences to the CSD system [10]. RC is a member of CONICET.

References

[1] A. Abragam, B. Bleaney, Electron Paramagnetic Resonance of Transition Ions, Clarendon Press, Oxford, 1970.
[2] J.A. Weil, J.R. Bolton, J.E. Wertz, Electron Paramagnetic Resonance. Elementary Theory and Practical Applications, Wiley, New York, 1993.
[3] C.A. Steren, R. Calvo, O.E. Piro, B.E. Rivero, Inorg. Chem. 28 (1989) 1933–1938.
[4] C.D. Brondino, N.M.C. Casado, M.C.G. Passeggi, R. Calvo, Inorg. Chem. 32 (1993) 2078–2084.
[5] S.D. Dalosto, M.G. Ferreira, R. Calvo, O.E. Piro, E.E. Castellano, J. Inorg. Biochem. 73 (1999) 151–155.
[6] M.B. Massa, S.D. Dalosto, M.G. Ferreyra, G. Labadie, R. Calvo, J. Phys. Chem. A 103 (1999) 2606–2617.
[7] S.K. Hoffmann, W. Hilczer, J. Goslar, M.B. Massa, R. Calvo, J. Magn. Reson. 153 (2001) 92–102.

[8] S.D. Dalosto, R. Calvo, J.L. Pizzaro, M.L. Arriortua, J. Phys. Chem. A 105 (2001) 1074–1085.
[9] F.S. Stephens, R.S. Vagg, P.A. Williams, Acta Crystallogr., Sect. B 33 (1977) 433–437.
[10] F.H. Allen, Acta Crystallogr., Sect. B 58 (2002) 380–388.
[11] F.S. Stephens, R.S. Vagg, P.A. Williams, Acta Crystallogr., Sect. B 31 (1975) 841–845.
[12] I. Vencato, C. Lariucci, K.D. Ferreira, R.C. Santana, J.F. Carvalho, Acta Crystallogr., Sect. E 60 (2004) m1428–m1430.
[13] S. Stoll, Spectral Simulations in Solid-state EPR, PhD Thesis (Zürich: ETH). EasySpin is available at http://www.esr.ethz.ch/EasySpin/home.html, 2003.
[14] S. Stoll, A. Schweiger, J. Magn. Reson. 178 (2006) 42–55.
[15] J.R. Pilbrow, Transition Ion Electron Paramagnetic Resonance, Clarendon Press, Oxford, 1990.
[16] R. Calvo, S.B. Oseroff, H.C. Abache, J. Chem. Phys. 72 (1980) 760–767.
[17] J.A. Weil, J. Magn. Reson. 18 (1975) 113–116.